

Detailed Comparison of Experimental Observations and Computer Tracking for the SPS Dynamic Aperture Experiment

W. Fischer*, M. Giovannozzi† and F. Schmidt
 CERN
 CH-1211 Geneva 23

Abstract

The design of large super-conducting hadron colliders relies heavily on the evaluation of the dynamic aperture through computer tracking. The SPS Dynamic Aperture Experiment provides an interesting test bench for such a technique. This experiment was set up to understand long-term stability of protons under the influence of strong non-linear fields in conjunction with tune ripple. Beam losses were investigated for two different working points far from low order resonances, for varying particle amplitudes, tune modulation frequencies and depths. Long-term multi-particle tracking simulating the actual distributions in the machine was performed in an effort to reproduce the main features of the SPS experiment. Mechanisms that lead to particle loss in long-term simulations are discussed.

1 INTRODUCTION

Computer tracking is a simple and flexible tool to follow particles in complex accelerator structures over many turns due to the ever faster computer facilities. It is therefore used in the design of large hadron colliders like LHC. However, it has never been shown how well simulations can predict the dynamic aperture for operating machines. Experiments are therefore needed to test the validity and limits of tracking in finding the dynamic aperture under controlled conditions. The SPS is basically a very linear machine which can be made non-linear by powering 8 strong sextupoles and in which an artificial tune modulation, stronger than the natural one due to the SPS power supplies can be introduced. The details of the experiments are described elsewhere [1, 2]. In the following only the main parameters are given: Two working points (Q_H, Q_V) are used,

- (26.637, 26.533), referred to as WP1,
- (26.605, 26.538), referred to as WP2;

the ripple frequencies are 9Hz, 40Hz and 180Hz with the modulation depth ΔQ of $0.55 \cdot 10^{-3}$ and $1.1 \cdot 10^{-3}$; the strongest resonances are ($8Q_h = 213$, $3Q_h + 4Q_v = 186$) and $5Q_h = 133$ at WP1 and WP2 respectively; potentially WP2 is more unstable than WP1.

The following procedure is used in the experiment: the beam is first kicked horizontally to approximately fill the dynamic aperture, then vertical scrapers remove the vertical halo and horizontal scrapers cut off 5 to 10% of the

particles (T_{-2} in Fig. 2) to define a clean beam edge. At T_{-1} the ripple is switched on and at T_0 the horizontal scraper is retracted by 1.4mm ($\beta_h = 100m$). We denote the end of the experimental session by T_1 .

In the next section we compare the long-term particle losses seen in experiment and simulations. Section 3 is devoted to the discussion of mechanisms that lead to particle loss.

2 SIMULATION OF PARTICLE LOSSES IN THE EXPERIMENT

Our aim is to reproduce the experimental intensity curves for the different ripple depths and modulation frequencies. For the time being we restrict ourselves to WP2 since contrary to WP1 we find sizeable particle losses already at 10^6 turns.

2.1 Method of Reconstruction

In our simulations “super particles” represent the actual particle distribution. These “super particles” are distributed in horizontal betatron amplitude r and momentum deviation $\delta = \Delta p/p$. The vertical distribution has only been treated approximately. The “super particles” produce the intensity curves when the proper weight according to the assumed initial distribution is attached.

The tracking starts at a location with small dispersion where we may factorize the distribution $f(r, \delta)$ as $f_r(r)f_p(\delta)$. For the horizontal betatron distribution $f_r(r)$ we assumed a Gaussian distribution with standard deviation σ before the kick. This leads to a distribution

$$f_r(r) = \frac{r}{\sigma^2} \exp \left\{ -\frac{a^2 + r^2}{2\sigma^2} \right\} I_0 \left(\frac{ar}{\sigma^2} \right), \quad (1)$$

after a kick a , where I_0 is the modified Bessel function of first kind and order zero. The distribution $f_p(\delta)$ of the momentum

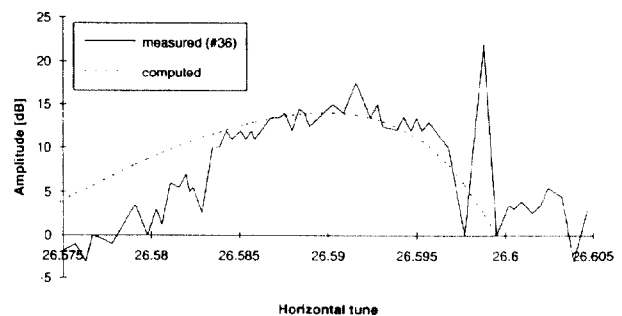


Figure 1: Measured and calculated horizontal tune distribution. Note that the amplitude scale is logarithmic.

*Supported in part by DESY Hamburg, Germany.

†Supported in part by INFN Sezione di Bologna, Italy.

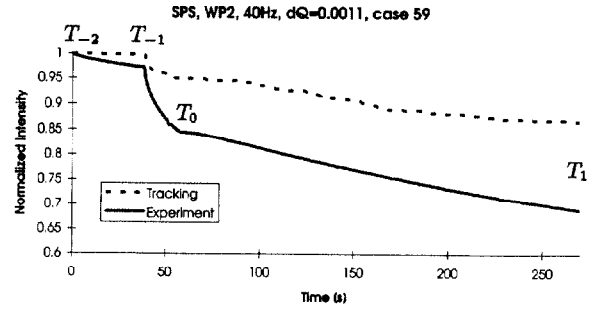
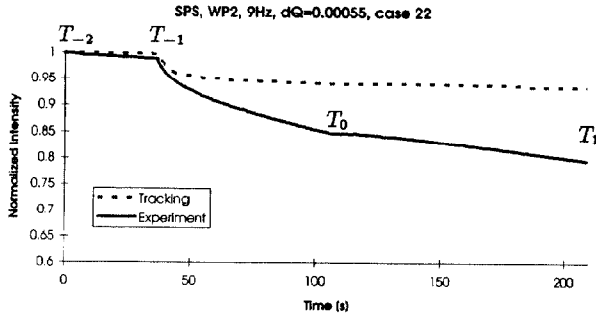


Figure 2: Reconstructed intensity curves for different parameters. Note that the vertical axis starts at 0.6.

deviation $\delta = \Delta p/p$ is represented by

$$f_p(\delta) = \frac{2}{\pi} \cos^2 \left(\frac{\pi}{2} \frac{\delta}{\delta_{max}} \right). \quad (2)$$

To justify the assumption of Eq. (1) we have multiplied the detuning curve $Q(r)$ (not shown in this report) with the distribution $f_p(r)$ and compared the result with the horizontal tune distribution obtained from the transverse Schottky signal (see Fig. 1). The overall agreement is satisfactory with the exception of the peak due to the 5th order resonance which is not included in the model. The longitudinal distribution $f_p(\delta)$ also agrees well with the longitudinal Schottky signal.

We used 180 particles to represent the experimental distribution. The three intervals $[T_{-2}, T_{-1}]$, $[T_{-1}, T_0]$ and $[T_0, T_1]$ were treated separately but the weights for lost particles were transferred into the next interval. In the last interval the particles are tracked up to 10 million turns.

2.2 Estimation of Statistical Errors

There are various types of errors. The first comes from the lack of statistics since we track 180 weighted particles instead of about 10^{12} particles in the experimental distribution.

Furthermore we use a certain number of experimental values for the reconstruction, all measured with a certain precision. To estimate the effect of these errors we varied the values under consideration by typically 5%, the results being listed in Tab. 1. The total error is given as the square root of the sum of squares of the individual errors.

Table 1: Error estimation for the intensity drop in the interval $[T_{-1}, T_0]$ by varying parameters

ΔQ	$0.55 \cdot 10^{-3}$	$1.1 \cdot 10^{-3}$
emittance ϵ	+3%/-6%	+3%/-6%
momentum width δ_{max}	+1%/-3%	+2%/-5%
kick strength a	+6%/-6%	+10%/-10%
scraper position	+3%/-12%	+3%/-11%
total	+8%/-14%	+12%/-17%

2.3 Results

Fig. 2 shows the comparison between the experimental and simulation results for $\Delta Q = 0.55 \cdot 10^{-3}$, 9Hz and $\Delta Q = 1.1 \cdot 10^{-3}$, 40Hz. Besides the above stated statistical error there is clearly a systematic underestimation of the losses in the simulations. Compared to the simulations the experimental intensities at T_1

are lower by 15% and 22% respectively. What is even more important is that the loss rates are by far more pronounced in the experiment. It has to be stated that much care has been applied in tracking investigations: all known phenomena are taken into account, the non-linear content of the SPS is very well reproduced leading to an excellent agreement of detuning versus amplitude curves $Q(r)$, and all aspects concerning distributions are faithfully addressed and checked meticulously (the nice agreement of Fig. 1 relies heavily on the last two points). A discussion on possible causes of this discrepancy is given in section 4.

3 DISCUSSION OF LOSS MECHANISMS

In parallel to comparing the experimental results with tracking we performed a detailed study of the mechanisms that lead to long-term particle loss in the simulations. We chose WP1, 9Hz and $\Delta Q = 1.1 \cdot 10^{-3}$ for these examinations. For the horizontal start amplitude we used 3 values and fixed the vertical amplitude to a probable mean value in all cases. The tracking was done with and without scraper. As all our starting amplitudes are located in the chaotic region we had to take many particles (640) concentrated them in a very small domain in phase space.

3.1 Methods

Firstly we applied the Lyapunov method to test the degree of chaoticity. We used a pair of close-by particles (initial phase space distance of 10^{-7} mm) and followed the evolution of their distance in time. In Tab. 2 we give the angular distance between those 2 particles after a given time. Secondly we used the averaged tune per ripple period to relate chaotic behaviour to resonances. Thirdly we averaged the amplitudes (again over one ripple period) and studied their mean and rms values as a function of time. Finally we created the standard survival plot using 3 million turns and derived the time dependent loss rate from it.

3.2 Results

In Fig. 3 all sum, skew and difference resonances up to order 13 are shown in the regime which is relevant for the motion for three selected amplitudes at WP1. The averaged tunes per ripple period are depicted together with the modulation depth. At the smallest amplitude (most to the right in Fig.3) the 8th order resonance is crossed due the tune modulation leading to

large fluctuations of the tunes. It is interesting to note that the tunes follow the detuning curve. The largest amplitude (most to the left in Fig.3) reaches the 7th order resonance.

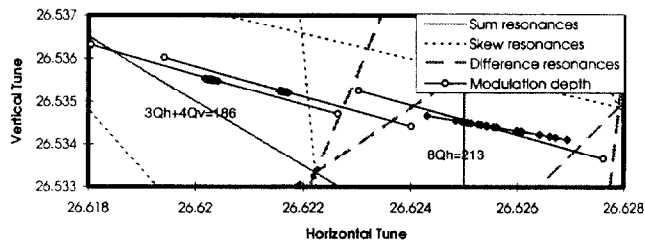


Figure 3: Averaged tunes per ripple period (squares) for the amplitudes 16.8, 18.8 and 19.5mm (right to left).

In Fig. 4 the amplitude of 32 particles, averaged over one ripple period, is shown for the largest amplitude value. As the particles are chaotic their amplitudes will spread slowly (in $10^5 - 10^6$ turns) and finally they will either reach the 7th order resonance, after which they are extracted in some 10^4 turns, or they are attracted by the 8th order resonance. The former takes place more rapidly (see Tab. 2) when the distribution is initially at larger amplitude and therefore closer to the 7th order resonance; the latter can be seen as an amplitude drop of one particle after 2.7 million turns.

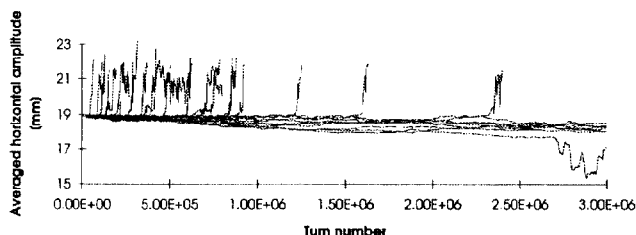


Figure 4: Amplitude evolution of 32 particles starting at $A_x = 19.5\text{mm}$ ($\beta_h = 100m$) under the influence of tune ripple of 9Hz and $\Delta Q = 1.1 \cdot 10^{-3}$. The amplitude is averaged over one ripple period.

Fig. 5 shows the evolution of the rms values of the 3 starting amplitudes as a function of time. At the smallest amplitude the trajectories fill quickly a broad band due to the presence of the 8th order resonance. Following the definition of smear for non-linear motion [3] the width of this band might be called “chaotic smear”. The difference in the “chaotic smear” of the 3 particles fits well to the chaotic behaviour shown in Tab. 2. The deviation from the smooth behaviour of the curves in Fig. 5, after 1.7 million and 2.7 million turns for the medium and large amplitude respectively, can be attributed to a decrease of the amplitudes for some particles which get attracted to the 8th order resonance.

Due to the large distance to the 7th order resonance the smallest amplitude particles, even though most chaotic, are not lost without scrapers (see Tab 2). Once an aperture limit is introduced (2.8mm from the start amplitude) it is reached preferably by the particles with the largest “chaotic smear” (see loss rate coefficients in Tab. 2), i.e. those close to the 8th order resonance.

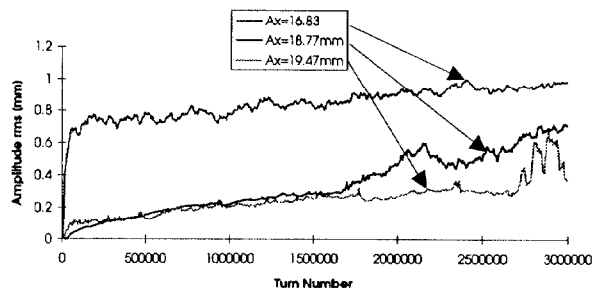


Figure 5: Time dependent amplitude rms values (“chaotic smear”) for three different starting amplitudes.

Table 2: Particle stability at three different starting amplitudes at WP1

horizontal amplitude [mm] at $\beta_h = 100m$	16.8	18.8	19.5
separation of 2 particles [π] after 20000 turns,	0.9	0.45×10^{-4}	0.8×10^{-3}
lost particle out of 640, no scraper	0	102	502
amplitude rms value [mm], after 20000 turn, no scraper	0.99	0.72	0.38
exponential coefficient of loss rate [10^{-4}], with scraper	-1.54	-0.80	-1.37

4 CONCLUSIONS

These studies have provided a better insight into the loss mechanisms due to non-linearities associated with tune ripple. However, a complete quantitative agreement between experiment and simulations has not yet been found. The large chaotic band revealed by tracking may explain the larger losses in the experiments since particles oscillating in these bands could reach the scraper even after its partial retraction. In the upcoming experiments we will therefore use the scrapers only to cut the beam halo and as a closest aperture limiter, whilst possible blow-ups will be studied with nondestructive wire scanners. Of course it can not be excluded that some unknown process has not been included yet in our simulations.

5 ACKNOWLEDGEMENTS

The authors would like to thank J. Gareyte for taking part in several experimental sessions and many helpful discussions.

6 REFERENCES

- [1] J. Gareyte, W. Scandale and F. Schmidt, “Review of the Dynamic Aperture Experiment at the CERN SPS”, in Proceedings of the International Workshop on Nonlinear Problems in Accelerator Physics, Berlin, 1992.
- [2] W. Fischer et al., “Recent Results from the Dynamic Aperture Experiment at the SPS”, in Proceedings of the 1993 IEEE Particle Accelerator Conference, Washington, D.C., 1993, pp. 246-248.
- [3] M. A. Furman and S. G. Peggs, “A Standard for the Smear”, SSC-N-634, 1989.